

Noise-Resistant Local Binary Pattern with an Embedded Error-Correction Mechanism

Jianfeng Ren, *Student Member, IEEE*, Xudong Jiang, *Senior Member, IEEE*, and Junsong Yuan, *Member, IEEE*

Abstract—Local binary pattern (LBP) is sensitive to noise. Local ternary pattern (LTP) partially solves this problem. However, both LBP and LTP treat the corrupted image patterns as they are. In view of this, we propose a noise-resistant LBP (NRLBP) to preserve the image local structures in presence of noise. The small pixel difference is vulnerable to noise. Thus, we encode it as an *uncertain* state first, and then determine its value based on the other bits of the LBP code. It is widely accepted that most image local structures are represented by uniform codes and noise patterns most likely fall into non-uniform codes. Therefore, we assign the value of *uncertain* bit so as to form possible uniform codes. In such a way, we develop an error-correction mechanism to recover the distorted image patterns. In addition, we find that some image patterns such as lines are not captured in uniform codes. Those line patterns may appear less frequently than uniform codes, but they represent a set of important local primitives for pattern recognition. Thus, we propose an extended noise-resistant LBP (ENRLBP) to capture line patterns. The proposed NRLBP and ENRLBP are more resistant to noise compared with LBP, LTP and many other variants. On various applications, the proposed NRLBP and ENRLBP demonstrate superior performance to LBP/LTP variants.

Index Terms—Local Binary Pattern, Local Ternary Pattern, Uniform Patterns, Noise Resistance.

I. INTRODUCTION

LOCAL binary pattern (LBP) operator transforms an image into an array or image of integer labels describing micro-pattern, i.e. pattern formed by a pixel and its immediate neighbors [1]. More specifically, LBP encodes the signs of the pixel differences between a pixel and its neighbouring pixels to a binary code. The histogram of such codes in an image block is commonly used for further analysis. It has been widely used in texture classification [2]–[10], dynamic texture recognition [11]–[13], facial analysis [14]–[21], human detection [22], [23] and many other tasks [24]–[33]. Its popularity arises from the following advantages. Firstly, the exact intensities are discarded, and only the relative intensities with respect to the center are preserved. Thus, LBP is less sensitive to illumination variations. Secondly, by extracting the histogram of micro-patterns in a patch, the exact location information is discarded, and only the patch-wise location information is preserved. Thus, LBP is robust to alignment

error. Lastly, LBP features can be extracted efficiently, which enables real-time image analysis.

Although LBP has gained much popularity because of its simplicity and robustness to illumination variations, its sensitivity to noise limits its performance [19]. In [3], uniform LBP was proposed to reduce the noise in LBP histogram. The LBP codes are defined as uniform patterns if they have at most two circularly bitwise transitions from 0 to 1 or vice versa, and non-uniform patterns if otherwise. In uniform LBP mapping, one separate histogram bin is used for each uniform pattern and all non-uniform patterns are accumulated in a single bin. Most LBPs in natural images are uniform patterns [3], [15]. Thus, uniform patterns are statistically more significant, and their occurrence probabilities can be more reliably estimated. In contrast, non-uniform patterns are statistically insignificant, and hence noise-prone and unreliable. By grouping the non-uniform patterns into one label, the noise in non-uniform patterns is suppressed. The number of patterns is reduced significantly at the same time.

In [7], [34]–[37], information in non-uniform patterns is extracted and also used for classification. Liao et al. proposed dominant LBP patterns that consider the most frequently occurred patterns in a texture image [7]. Zhou et al. [34] and Fathi et al. [35] proposed to extract information from non-uniform patterns based on pattern uniformity measure and the number of ones in the LBP codes. Principal Component Analysis [36] and random subspace approach [37] were utilized to extract information from the whole LBP histogram including both uniform patterns and non-uniform patterns. These approaches extract some useful information from non-uniform codes. However, they tend to be sensitive to noise.

“Soft histogram” is another approach to improve the robustness to noise, e.g. a fuzzy LBP (FLBP) using piecewise linear fuzzy membership function [5], [28] and another using Gaussian-like membership function [18]. A comprehensive comparison between LBP and fuzzy LBP in classifying and segmenting textures is given in [38]. Instead of hard-coding the pixel difference, a probability measure is utilized to represent its likelihood as 0 or 1. However, the probability is closely related to the magnitude of the pixel difference. Thus, it is still sensitive to noise.

Local ternary pattern (LTP) was proposed in [19] to tackle the image noise in uniform regions. Instead of binary code, the pixel difference is encoded as a 3-valued code according to a threshold t . Then, the ternary code is split into a positive LBP and a negative LBP in order to reduce the dimensionality. LTP was shown less sensitive to noise, especially in uniform regions [19]. Subsequently, many LTP variants were proposed

Copyright (c) 2013 IEEE. Personal use of this material is permitted. However, permission to use this material for any other purposes must be obtained from the IEEE by sending a request to pubs-permissions@ieee.org.

J. Ren is with BeingThere Centre, Institute of Media Innovation, Nanyang Technological University, 50 Nanyang Drive, Singapore 637553. (e-mail: jfren@ntu.edu.sg).

X. Jiang and J. Yuan are with School of Electrical & Electronics Engineering, Nanyang Technological University, 50 Nanyang Avenue, Singapore 639798. (e-mail: {exdjiang, jsyuan}@ntu.edu.sg)

in the literature. Nanni et al. proposed a quinary code of five values according to two thresholds [31], and then split it into four binary codes similarly as LTP. As LTP is not invariant under scaling of intensity values, Liao et al. proposed Scale Invariant Local Ternary Pattern to deal with the gray scale intensity changes in a complex background [32]. In order to reduce the high dimensionality of LTP, Center-Symmetric LTP was proposed in [33]. Instead of the pixel difference between the neighboring pixel and the central pixel, the pixel difference between diagonal neighbors is calculated. In Local Adaptive Ternary Patterns [20] and extended LTP [9], instead of using a constant threshold, the threshold is calculated for each window using some local statistics, which makes them less sensitive to illumination variations. In Local Triplet Pattern [30], the equality is modeled as a separate state, and a tri-state pattern is formulated. It can be viewed as a special case of LTP [19].

LTP and its variants partially solve the noise-sensitive problem. However, they lack a mechanism to recover the corrupted image patterns. In this paper, we propose a Noise-Resistant LBP (NRLBP) and an Extended Noise-Resistant LBP (ENRLBP) to address this issue.

The signs of pixel differences used to compute LBP and its variants are vulnerable to noise when they are small. Thus, we propose to encode small pixel difference as an *uncertain* bit first and then determine its value based on the other bits of the LBP code. Uniform patterns are more likely to occur compared with non-uniform patterns in natural images [3], [15]. Most image structures are represented by uniform patterns, and non-uniform patterns are most likely caused by noise. Thus, in the proposed NRLBP, we assign the values of *uncertain* bits so as to form uniform patterns. A non-uniform pattern is generated only if no uniform pattern can be formed. As noise may change an uniform pattern into an unstable non-uniform pattern, the proposed NRLBP corrects many distorted non-uniform patterns back to uniform patterns.

For LBP and LTP, line patterns are treated as non-uniform patterns and grouped into the non-uniform bin. Uniform patterns mainly represent spot, flat region, edge, edge end and corner. A local image is a line pattern if it is a line against the background, as shown in Fig. 5. Line patterns may appear less frequently than uniform patterns, but they represent an important group of local primitives for pattern recognition. Thus, we propose an extension set of uniform patterns corresponding to line patterns. Then, we propose extended noise-resistant LBP (ENRLBP). During the encoding process, we assign the values of *uncertain* bits so as to form extended uniform patterns.

To evaluate our approaches, we first inject Gaussian noise and uniform noise of different noise levels on the AR database [39] for face recognition and the Outex dataset [40] for texture recognition. The proposed approaches demonstrate strong resistance to noise compared with LBP/LTP and its variants. The proposed approaches are further compared with LBP/LTP variants for face recognition on the extended Yale database [41], [42] and the O2FN database [43], protein cellular classification on the 2D HeLa database and image segmentation on the Outex dataset [40] and also a natural image downloaded from the web. The proposed NRLBP and

ENRLBP consistently achieve comparable or better performance compared with LBP/LTP and its variants.

II. NOISE-RESISTANT LBP

A. Problem Analysis of LBP and LTP

Local binary pattern encodes the pixel difference $z_p = i_p - i_c$ between the neighboring pixel i_p and the central pixel i_c . Let $C_{P,R}^B = \overrightarrow{b_{P-1}^B b_{P-2}^B \dots b_1^B b_0^B}$ denote the LBP code of P neighbors at the distance of R to the center pixel. A code is also called a pattern. Let $LBP_{P,R}$ denote such a coding scheme for $C_{P,R}^B$. Each bit is obtained as:

$$b_p^B = \begin{cases} 1 & \text{if } z_p \geq 0, \\ 0 & \text{if } z_p < 0. \end{cases} \quad (1)$$

LBP is widely used in many applications because of its simplicity and robustness to illumination variations. However, LBP is sensitive to image noise. In [3], uniform LBP was proposed to capture fundamental image structures and reduce the noise in LBP histogram. The uniformity U is defined as the number of circularly bitwise transitions from 0 to 1 or vice versa. A local binary pattern is $u2$ -uniform or simply called uniform if $U \leq 2$. For example, “11110000” is a uniform pattern as $U = 2$, whereas “01010111” shown in Fig. 1(a) is a non-uniform pattern as $U = 6$. $LBP_{P,R}^{u2}$ indicates a coding and histogram mapping scheme in which $u2$ -uniform LBP codes of P neighbors at the distance of R to the center pixel are utilized. Uniform patterns occur much more frequently than non-uniform patterns in natural images. It has been shown that $LBP_{8,1}^{u2}$ accounts for almost 90% of all patterns for texture images [3] and $LBP_{8,2}^{u2}$ accounts for 90.6% for facial images [15]. The occurrence probabilities of non-uniform patterns are so small that they cannot be reliably estimated [3]. Inclusion of such noisy estimates in the histogram would harm the classification performance. In addition, non-uniform patterns may be caused by the image noise. Therefore, when constructing the histogram, all non-uniform patterns are grouped into one bin. This not only reduces feature dimensionality, but more importantly, the noise due to unreliable estimates of non-uniform patterns is greatly suppressed. The number of patterns is reduced significantly from 2^P to $P(P-1)+3$. For example, $LBP_{8,2}$ consists of 256 patterns whereas $LBP_{8,2}^{u2}$ has only 59 patterns.

Uniform LBP successfully reduces the noise in LBP histogram, but it is still sensitive to image noise. As shown in Fig. 1(a), a small noise will cause the pixel difference encoded differently. Ideally such a smooth region should be encoded as “11111111”. Due to the image noise, it is encoded as “01010111” instead. LTP partially solves this problem by encoding the small pixel difference into a third state [19]. Instead of using binary code, each pixel difference is encoded as a 3-valued code. Let $C_{P,R}^T = \overrightarrow{b_{P-1}^T b_{P-2}^T \dots b_1^T b_0^T}$ denote the LTP code of P neighbors at the distance of R to the center pixel and $LTP_{P,R}$ denote such a coding scheme for $C_{P,R}^T$.

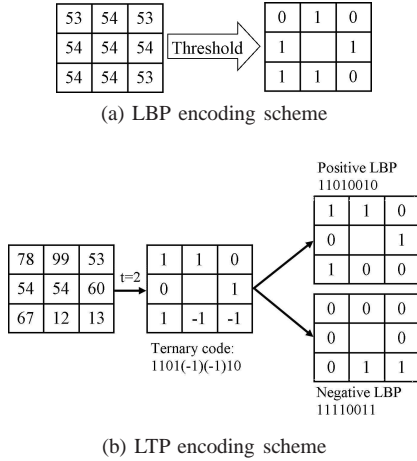


Fig. 1. (a) An example of LBP encoding scheme for the smooth region with small image noise. LBP is sensitive to image noise. (b) An example of LTP encoding process. LTP doubles the number of patterns compared with LBP.

Each bit is obtained as:

$$b_p^T = \begin{cases} 1 & \text{if } z_p \geq t, \\ 0 & \text{if } |z_p| < t, \\ -1 & \text{if } z_p \leq -t, \end{cases} \quad (2)$$

where t is a pre-defined threshold.

LTP is more resistant to noise. However, the dimensionality of LTP histogram is very large, e.g. $LTP_{8,2}$ exhibits a histogram of $3^8 = 6561$ bins. Thus, in [19], LTP is split into a positive LBP and a negative LBP. Each bit of positive LBP is obtained as:

$$b_p^p = \begin{cases} 1 & \text{if } z_p \geq t, \\ 0 & \text{if } z_p < t. \end{cases} \quad (3)$$

Each bit of negative LBP is obtained as:

$$b_p^n = \begin{cases} 0 & \text{if } z_p \leq -t, \\ 1 & \text{if } z_p > -t. \end{cases} \quad (4)$$

To show the commonalities and differences among LBP, LTP and the proposed NRLBP clearly, the negative LBP defined here is the complement of the negative LBP defined in [19]. Effectively they achieve the same result for histogram-based comparison. Eventually, LTP is treated as two separate channels of LBP codes: one channel for positive LBP and the other for negative LBP. In general, uniform LTP is used, in which both channels are uniform LBP. This coding scheme is denoted by $LTP_{P,R}^{u,2}$. An example of LTP encoding process is shown in Fig. 1(b). LTP doubles the number of patterns compared with LBP.

The small pixel difference may be easily distorted by the noise. Both LBP and LTP lack a mechanism to correct the corrupted patterns. The corrupted image patterns are treated without any attempt to recover the underlining local structures. To address this issue, we propose a Noise-Resistant LBP and an Extended Noise-Resistant LBP.

B. Proposed Noise-Resistant LBP

LBP is sensitive to noise. Even a small noise may change the LBP code significantly. Thus, we propose to encode the

small pixel difference as an *uncertain* bit X first and then determine X based on other certain bits of the LBP code. For the pixel difference z_p between the neighboring pixel and the central pixel, we encode it into one of the three states b_p^N as:

$$b_p^N = \begin{cases} 1 & \text{if } z_p \geq t, \\ X & \text{if } |z_p| < t, \\ 0 & \text{if } z_p \leq -t. \end{cases} \quad (5)$$

States 1 and 0 represent two strong states where the pixel difference is almost definitely positive and negative, respectively. Noise can unlikely change them from 0 to 1 or from 1 to 0 . State X represents an *uncertain* state where the pixel difference is small. A small pixel difference is vulnerable to noise if we only take its sign. More specifically, noise can easily change its LBP bit from 0 to 1 or vice versa. Therefore, we encode it as an *uncertain* state regardless its sign.

Then, we constrain the value of the *uncertain* bit into either 0 or 1 , represented by a variable $x_i, x_i \in \{0, 1\}$. Let $\mathbf{X} = (x_1, x_2, \dots, x_n)$ denote the vector formed by n variables of a code. $\mathbf{X} \in \{0, 1\}^n$. The *uncertain* code can be represented by $C(\mathbf{X})$ as:

$$\overrightarrow{b_{P-1}^N b_{P-2}^N \dots b_1^N b_0^N} = C(\mathbf{X}). \quad (6)$$

Take the *uncertain* code “11X100X0” in Fig. 2(a) for illustration. The *uncertain* code $\overrightarrow{11x_2100x_10}$ can be viewed as the function of $\mathbf{X} = \{x_1, x_2\}$.

After we derive the *uncertain* code, we determine the *uncertain* bits based on the values of the other certain bits to form one or more codes of image local structures. Uniform patterns represent local primitives, including spot, flat, edge, edge end and corner. They appear much more often than non-uniform patterns in natural images. Since uniform patterns occur more likely than non-uniform ones, we assign the values of *uncertain* bits \mathbf{X} so as to form possible uniform LBP codes. A non-uniform pattern is generated only if no uniform pattern can be formed. Take Fig. 2(b) as an example. We determine the *uncertain* bit of *uncertain* code “11X1X0X0” so as to form only uniform patterns, e.g. “11110000” and “11111000”.

Mathematically, let Φ_u denote the collection of all uniform LBP codes. For $LBP_{8,2}^{u,2}$, Φ_u consists of 58 uniform codes. Based on the *uncertain* code $C(\mathbf{X})$, a set of the proposed NRLBP codes are obtained as:

$$S_{NRLBP} = \{C(\mathbf{X}) | \mathbf{X} \in \{0, 1\}^n, C(\mathbf{X}) \in \Phi_u\} \quad (7)$$

Now let us construct the histogram of NRLBP for a local image patch. Let m denote the number of elements in S_{NRLBP} . If $m > 0$, the bin corresponding to each element in S_{NRLBP} will be added by $1/m$. After all, all these patterns originate from one *uncertain* code. If $m = 0$, the non-uniform bin will be added by 1. This process is repeated for every pixel in the patch. Algorithm 1 summarizes the process.

Now we compare the proposed NRLBP with LBP and LTP by several examples. We consider the cases that different number of LBP codes are derived in S_{NRLBP} . Image patterns in Fig. 2(a), (b), (c), (d) generate $m = 1, 2, 3, 4$ NRLBP codes, respectively. Fig. 2(e) shows an example where no uniform code can be formed for NRLBP. The corresponding LBP code

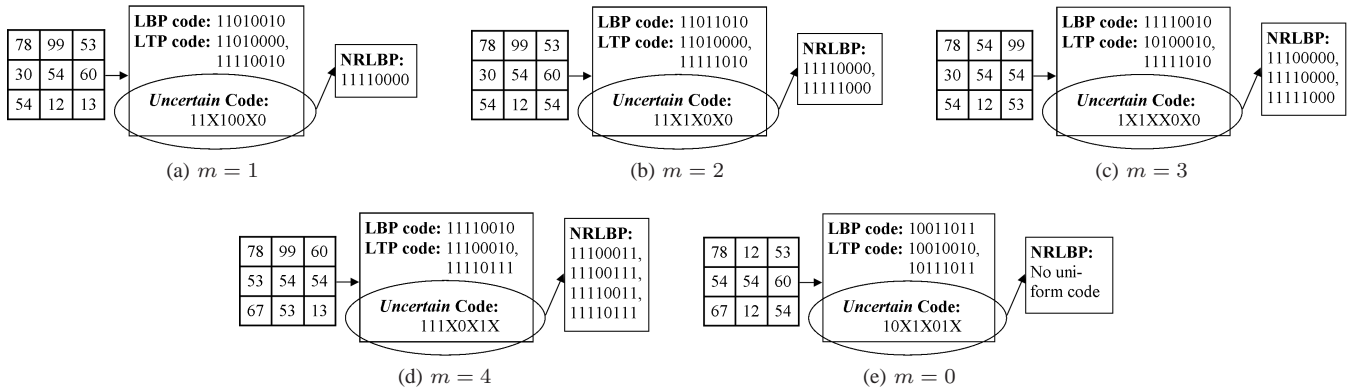


Fig. 2. Illustration of encoding process of NRLTP and comparison to LBP and LTP. Fig. (a), (b), (c), (d) are corresponding to $m = 1, 2, 3, 4$ resulting NRLBP codes, respectively. Fig. (e) shows an example that no uniform code can be formed. The proposed NRLBP is significantly different from LBP and LTP. Threshold t is chosen as 2 for LTP and NRLBP in this figure.

Algorithm 1 Histogram construction of the proposed NRLBP

for Every pixel in a patch **do**
 1. Derive the *uncertain* code $C(\mathbf{X})$ as in Eqn. (5), (6).
 3. Search *uncertain* bits \mathbf{X} in the space $\{0, 1\}^n$ so that $C(\mathbf{X})$ forms uniform LBP codes as in Eqn. (7).
 4. Construct the histogram.
if $m = 0$ **then**
 Accumulate the non-uniform bin with 1.
else
 Accumulate the bin of each pattern in S_{NRLBP} with $1/m$.
end if
end for

and LTP code are also given. For LTP, the positive LBP and negative LBP are accumulated in two different histograms, whereas for LBP and NRLBP, the codes are accumulated in one histogram.

As noise may change a uniform image pattern into an unstable non-uniform pattern, the proposed NRLBP corrects such a code back to uniform code. As shown in Fig. 2(a), the LBP code is “11010010”, which may be distorted by the noise. The proposed NRLBP first derives the *uncertain* code “11X100X0”, and then determine its *uncertain* bits by forming the uniform code “11110000”. This can be viewed as an error-correction mechanism. Note that we only attempt such an error correction on *uncertain* bits. We do not attempt to correct the non-uniform patterns that are resulted from two strong states. Similarly, we can observe such an error-correction process in Fig. 2(b), (c), (d). In these three cases, more than one NRLBP code is generated.

The proposed NRLBP corrects noisy non-uniform patterns back to uniform pattern. Fig. 3 shows the histogram of LBP, LTP and NRLBP for the image shown in Fig. 6(c). The threshold t is chosen as 10 for LTP and NRLBP. LTP histogram is the concatenation of positive LBP histogram and negative LBP histogram. The last bin of each histogram is corresponding to non-uniform patterns, and other bins are corresponding to uniform patterns. Clearly, compared with LBP histogram and LTP histogram, non-uniform patterns in

NRLBP histogram are reduced significantly from about 35% to about 10% only. The proposed NRLBP corrects a large amount of non-uniform patterns that are corrupted by the noise back to uniform patterns.

The proposed NRLBP is different from LBP and LTP in many other aspects besides the capability of noise resistance and error-correction. The LBP code is one of the NRLBP code set if it is uniform. The only exception is that the LBP code is non-uniform and is corrected back to uniform code in NRLBP. Compared with LTP, the treatment of *uncertain* state is totally different for NRLBP. For LTP, all *uncertain* bits are set to 0 for positive half and 1 for negative half as shown in Fig. 2, whereas for the proposed NRLBP, we do not hurry for a decision of the *uncertain* bits. We treat them as if they could be encoded as 1 and/or 0, and determine their values based on the other bits of the code. Mathematically, for LTP, $\mathbf{X} \in \{0\}^n$ for positive half and $\mathbf{X} \in \{1\}^n$ for negative half, whereas $\mathbf{X} \in \{0, 1\}^n$ for NRLBP. The number of histogram bin is also different. LTP histogram consists of 118 bins, whereas NRLBP histogram only has 59 bins.

For implementation, a look-up table from the *uncertain* code to the feature vector of NRLBP histogram can be pre-computed. Then, the feature vector of local image patch can be easily obtained by summing up the feature vector of each pixel in this image patch.

C. Proposed Extended Noise-Resistant LBP

The local primitives represented by uniform LBP mainly consists of spots, flat region, edges, edge ends and corners [1], as shown in Fig. 4. However, a large group of local primitives are totally discarded, e.g. lines patterns, as shown in Fig. 5. Although those patterns may not appear as frequently as uniform patterns, they represent an important group of local primitives that may be crucial for recognition tasks. Grouping them with other non-uniform patterns into one bin may result in information lost. Therefore, we introduce an extended set of uniform patterns to preserve line patterns. Among all possible line patterns, diagonal lines appear less frequently. In order to keep the feature vector compact, we only choose nearly horizontal or vertical lines.

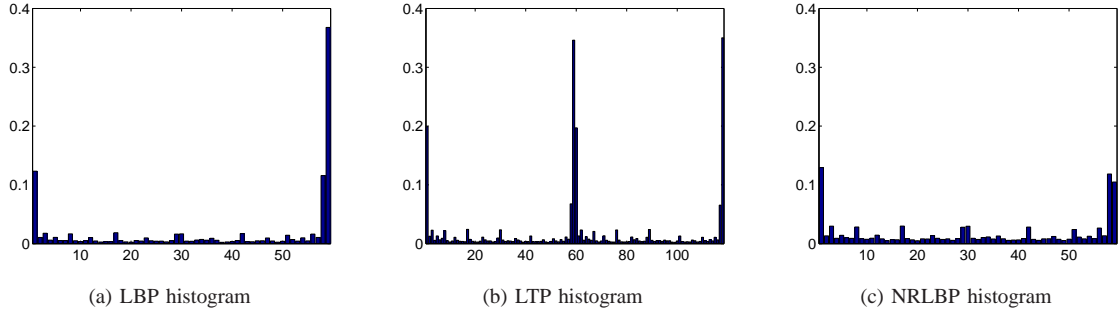


Fig. 3. The histogram of LBP, LTP and NRLBP for the image shown in Fig. 6(c). LTP histogram is the concatenation of positive LBP histogram and negative LBP histogram. The last bin of each histogram is corresponding to non-uniform patterns. Compared with LBP histogram and LTP histogram, NRLBP significantly reduces non-uniform patterns from about 35% to about 10%. The proposed NRLBP corrects a large amount of noisy non-uniform patterns back to uniform patterns.

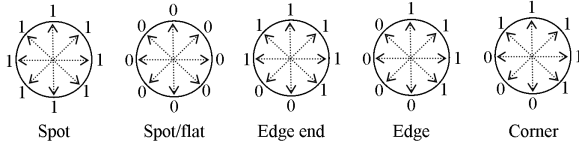


Fig. 4. Local primitives detected by $LBP_{8,2}^{u2}$.

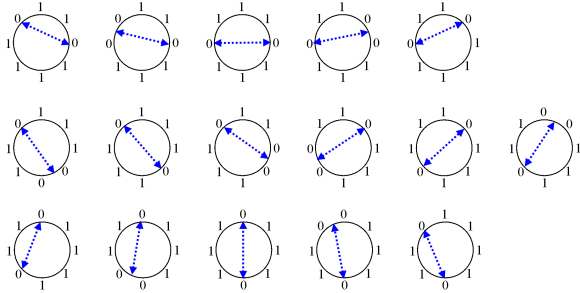


Fig. 5. Samples of line patterns. Those three rows are corresponding to horizontal, diagonal and vertical lines. The diagonal lines are rare patterns for natural images and hence discarded. The remaining horizontal and vertical lines are the proposed extended set of uniform patterns.

Let α denote the angle of the line away from the horizontal line. If $\alpha \in [0, 30^\circ]$ or $\alpha \in [150^\circ, 180^\circ]$, it is considered as a horizontal line. If $\alpha \in [60^\circ, 120^\circ]$, it is considered as a vertical line. If $\alpha \in [30^\circ, 60^\circ]$ or $\alpha \in [120^\circ, 150^\circ]$, it is considered as a diagonal line. Fig. 5 shows some samples of horizontal, diagonal and vertical lines.

The proposed extended set of uniform patterns consist of 48 patterns. Including 58 uniform patterns, we derive the extended uniform patterns. Similarly as NRLBP, we can derive the extended NRLBP (ENRLBP). Instead of forming uniform patterns, we form extended uniform patterns as our ENRLBP pattern. In such a way, line patterns are preserved during the encoding process. The number of bins of ENRLBP histogram is 107, which is smaller than LTP histogram that has 118 bins.

III. EXPERIMENTAL RESULTS

We conduct comprehensive experiments to validate the advantages of the proposed NRLBP and ENRLBP. Table I summarizes the approaches compared with, the classifiers used and the applications tested on. The proposed approaches

are compared with uniform LBP and uniform LTP. E.g. for face recognition, $LBP_{8,2}^{u2}$ and $LTP_{8,2}^{u2}$ are used. Let $NRLBP_{P,R}$, $ENRLBP_{P,R}$ denote the coding schemes for NRLBP and ENRLBP using P neighbors at the distance of R to the center pixel, respectively. The number of features for each patch is 59 for $LBP_{8,2}^{u2}$, 118 for $LTP_{8,2}^{u2}$, 59 for $NRLBP_{8,2}$ and 107 for $ENRLBP_{8,2}$. Dominant LBP (DLBP) [7], novel extended LBP (NELBP) [34] and noise tolerant LBP (NTLBP) [35] are compared as they extract information from non-uniform bins, similarly as our approaches do. We choose the dominant patterns that account for 80% of the total pattern occurrences, same as in [7]. Fuzzy LBP (FLBP) [5], [28], [38] is also compared. We implement fuzzy LBP using piece-wise linear fuzzy membership function in [5]:

$$f_{1,d}(z_p) = \begin{cases} 0 & \text{if } z_p < -d, \\ 0.5 + \frac{0.5z_p}{d} & \text{if } -d \leq z_p \leq d, \\ 1 & \text{if } z_p > d. \end{cases} \quad (8)$$

$$f_{0,d}(z_p) = 1 - f_{1,d}(z_p). \quad (9)$$

where $f_{1,d}$ and $f_{0,d}$ are the probability that pixel difference z_p should be encoded as 1 and 0, respectively. The parameter d controls the amount of fuzzification.

Different classifiers are utilized in our experiments. For face recognition, we use the nearest-neighbor (NN) classifier with three different distance measures: Chi-square distance, histogram intersection distance and G-statistic, as defined in Eqn. (10), (11) and (13), respectively. For texture recognition and protein cellular classification, linear SVM is used, and for image segmentation, k-means clustering algorithms is used.

$$\chi^2(\mathbf{x}, \mathbf{y}) = \sum_{i,j} \frac{(x_{i,j} - y_{i,j})^2}{x_{i,j} + y_{i,j}}, \quad (10)$$

$$D_{HI}(\mathbf{x}, \mathbf{y}) = - \sum_{i,j} \min(x_{i,j}, y_{i,j}), \quad (11)$$

$$D_G(\mathbf{x}, \mathbf{y}) = - \sum_{i,j} x_{i,j} \log y_{i,j}, \quad (12)$$

where \mathbf{x}, \mathbf{y} are the concatenated LBP feature vectors of two image samples; $x_{i,j}$ and $y_{i,j}$ are j -th dimension of i -th patch.

TABLE I
SUMMARY OF THE APPROACHES COMPARED WITH, THE CLASSIFIERS USED AND THE APPLICATION TESTED ON.

The approaches	The classifier	The applications
LBP [2]	Nearest-neighbor classifier + Chi-square distance	Face recognition on the AR database [39]
LTP [19]	Nearest-neighbor classifier + histogram intersection distance	Face recognition on the extended Yale B database [41], [42]
Dominant LBP [7]	Nearest-neighbor classifier + modified G-statistic	Face recognition on the O2FN database [43]
Fuzzy LBP [5], [28], [38]	Linear SVM	Texture Recognition on the Outex-13 dataset [40]
Novel extended LBP [34]	K-means clustering	Protein cellular classification on the 2D Hela database [44]
Noise tolerant LBP [35]		Image segmentation on the Outex segmentation dataset [40]

The G-statistic is numerically unstable, as many histogram bins may have zero elements, which easily causes $D_G \rightarrow \text{inf}$. Thus, we modify it into a numerically stable form:

$$D_G(\mathbf{x}, \mathbf{y}) = - \sum_{i,j} x_{i,j} \log(x_{i,j} + y_{i,j}), \quad (13)$$

Only when both $x_{i,j}$ and $y_{i,j}$ are zero, we set $0 \log(0) = 0$. We call this distance measure as Modified G-statistic (MG). MG is numerically more stable and hence can better handle the problem of too few elements in the histogram than G-statistic.

We conduct comparison experiments for various applications. Firstly, we inject Gaussian noise and uniform noise of various noise levels onto the images of the AR database [39] for face recognition and the Outex-13 dataset [40] for texture recognition. The proposed NRLBP and ENRLBP are compared with various LBP/LTP variants in order to validate the noise-resistance property of the proposed approaches. Then, we apply the proposed approaches on real images that are noise-prone. Illumination variation is one of big challenges for face recognition. We conduct experiments on two challenge face databases with large illumination variations: the extended Yale B database [41], [42] and the O2FN database [43]. The proposed approaches are also compared with LBP/LTP variants for protein cellular classification on the 2D Hela database [44] and image segmentation on the image of the Outex segmentation database [40] and one image from the web. In order to reduce the illumination variations, the images of the Outex-13 dataset, the extended Yale B database and the O2FN database are pre-processed similarly as in [19]. We utilize the source codes provided by the authors of [19] to perform this photometric normalization.

A. Face Recognition on the AR Database

For face recognition, we adopt a challenging experimental setting. Only one image per subject is used as the gallery (or training) set and all others are used as the probe set. In many real applications, we are not able to obtain multiple images per subject and we may have only one image per subject.

On the AR database, the proposed approaches are compared with LBP/LTP variants on images injected with noise in order to demonstrate their noise-resistant property. The AR database is of high resolution and high image quality, and considered as a face database with almost no image noise. 75 subjects are chosen from the AR database, each with 14 images. For each subject, it contains images from 2 sections. Each section contains 7 images: one neutral image, 3 images with different facial expressions and 3 images in different illumination conditions. We repeat experiments 6 times. For

each trial, we use Image 1, 5, 6, 8, 12, 13 of each subject as the gallery set, respectively. The other 13 images of each subject are used as the probe set. It is a challenging experimental setting as face images with facial expression variations need to be identified just based on a single face image.

1) *Resistant to Additive Gaussian Noise*: Gaussian noise is one of the most common types of noise. The images are normalized in the range of $(0, 1)$, and then we apply additive Gaussian noise with zero mean and standard derivation of σ . We conduct the experiments for $\sigma = 0.05, 0.10, 0.15$. The samples of noisy images are shown in Fig. 6. When the noise level is high, the images are barely recognizable, and the recognition task becomes more challenging.

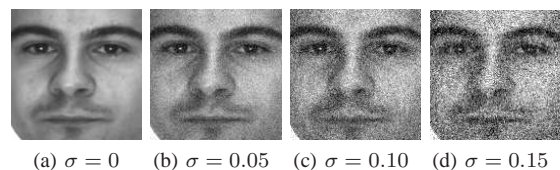


Fig. 6. The images with additive Gaussian noise of $\sigma = 0, 0.05, 0.1, 0.15$, respectively.

For LTP, NRLBP and ENRLBP, there is one free parameter: threshold $t \in [0, 255]$. Fuzzy LBP also has a free parameter: fuzzification d . We vary t for LTP, NRLBP and ENRLBP, and d for fuzzy LBP. Only the recognition rates at the optimal setting are reported. Table II summarizes the average recognition rate and the standard derivation of each approach at the optimal setting on the AR database injected with Gaussian noise. Table II shows that the proposed NRLBP and ENRLBP achieve comparable or slightly better performance compared with FLBP, whereas consistently outperform other approaches for all settings using different distance measures. As the noise level increases, the performance gain of the proposed approaches over approaches other than FLBP becomes more significant.

In order to study the effect of threshold t (or fuzzification parameter d), we plot the recognition rates vs. t (or d) for LTP, FLBP, NRLBP, ENRLBP using Chi-square distance, as shown in Fig. 7. LBP and DLBP are shown as dashed lines. For the low noise level, $\sigma = 0.05$, NRLBP and ENRLBP are slightly better than DLBP and visibly better than LBP, LTP and FLBP. For the middle noise level, $\sigma = 0.10$, the two proposed approaches slightly outperform FLBP and significantly outperform LBP, LTP and BLBP. For the high noise level, $\sigma = 0.15$, while LBP, LTP and DLBP fail to work, FLBP, NRLBP and ENRLBP can still achieve recognition rates over 70% if proper thresholds are applied. Fig. 7 shows

TABLE II
SUMMARY OF THE AVERAGE RECOGNITION RATE AND THE STANDARD DERIVATION OF EACH APPROACH AT THE OPTIMAL SETTING ON THE AR DATABASE INJECTED WITH GAUSSIAN NOISE.

Algorithm	Chi-square Distance, $\sigma =$			Histogram Intersection, $\sigma =$			Modified G-Statistics, $\sigma =$		
	0.05	0.10	0.15	0.05	0.10	0.15	0.05	0.10	0.15
LBP	83.44% $\pm 1.44\%$	64.65% $\pm 2.92\%$	40.91% $\pm 6.52\%$	81.64% $\pm 1.58\%$	55.18% $\pm 7.37\%$	34.34% $\pm 4.38\%$	79.04% $\pm 1.71\%$	56.63% $\pm 3.02\%$	34.56% $\pm 5.93\%$
LTP	83.91% $\pm 1.03\%$	65.09% $\pm 5.88\%$	43.78% $\pm 9.96\%$	81.85% $\pm 2.08\%$	55.26% $\pm 12.07\%$	37.69% $\pm 10.77\%$	80.26% $\pm 0.90\%$	62.58% $\pm 2.44\%$	42.74% $\pm 3.74\%$
DLBP	85.11% $\pm 0.83\%$	62.82% $\pm 6.92\%$	39.57% $\pm 9.76\%$	85.47% $\pm 1.74\%$	62.44% $\pm 7.09\%$	39.03% $\pm 9.87\%$	84.24% $\pm 1.68\%$	61.26% $\pm 5.46\%$	33.49% $\pm 9.04\%$
FLBP	83.95% $\pm 1.32\%$	78.19% $\pm 1.08\%$	71.04% $\pm 1.70\%$	84.17% $\pm 1.42\%$	74.26% $\pm 2.01\%$	59.86% $\pm 3.06\%$	81.44% $\pm 1.41\%$	74.97% $\pm 1.45\%$	68.77% $\pm 2.14\%$
NELBP	65.50% $\pm 3.19\%$	34.82% $\pm 3.01\%$	18.32% $\pm 1.35\%$	64.46% $\pm 3.84\%$	31.56% $\pm 1.81\%$	16.32% $\pm 1.07\%$	66.51% $\pm 3.27\%$	34.85% $\pm 2.23\%$	17.85% $\pm 1.69\%$
NLBP	63.71% $\pm 3.32\%$	28.94% $\pm 1.53\%$	13.42% $\pm 1.48\%$	67.25% $\pm 3.37\%$	35.69% $\pm 2.85\%$	17.83% $\pm 1.44\%$	61.01% $\pm 3.40\%$	25.35% $\pm 1.62\%$	11.47% $\pm 1.64\%$
NRLBP	85.33% $\pm 1.43\%$	79.93% $\pm 0.79\%$	70.67% $\pm 2.90\%$	85.88% $\pm 0.96\%$	78.65% $\pm 1.22\%$	67.62% $\pm 4.87\%$	84.92% $\pm 1.29\%$	79.08% $\pm 1.03\%$	70.55% $\pm 3.22\%$
ENRLBP	85.98% $\pm 1.35\%$	80.43% $\pm 0.97\%$	71.71% $\pm 1.79\%$	86.02% $\pm 1.09\%$	80.24% $\pm 1.55\%$	68.77% $\pm 3.05\%$	85.42% $\pm 1.03\%$	80.58% $\pm 0.72\%$	72.43% $\pm 1.50\%$

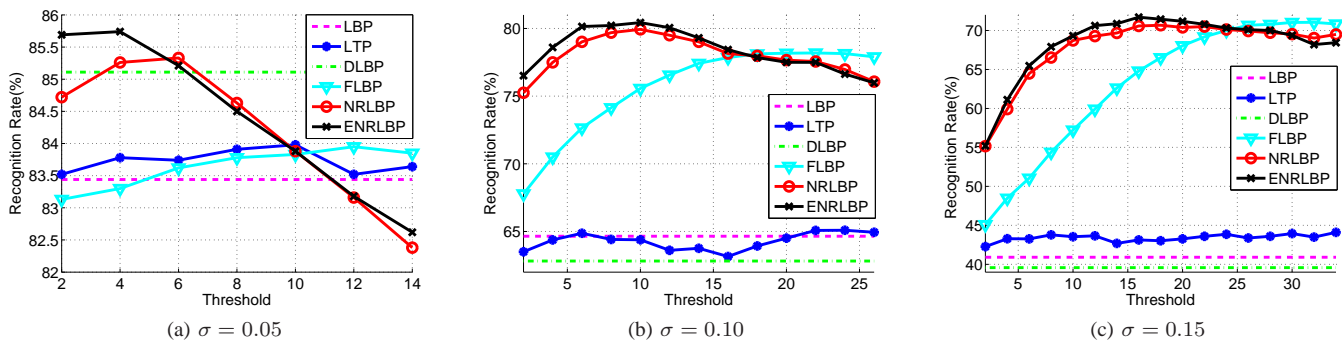


Fig. 7. The recognition rates of LBP, LTP, DLBP, FLBP, NRLBP and ENRLBP using Chi-square distance vs. threshold t on the AR database injected with Gaussian noise $\sigma = 0.05, 0.10, 0.15$. As the noise level increases, the optimal threshold increases.

that the two proposed approaches and FLBP are the only ones that work well for all tested noise levels.

We can also observe from Fig. 7 that the optimal threshold increases when the noise level increases. The gradual change of face image carries important information, and will result in small pixel differences. A small threshold will be sufficient to handle the small image noise. If the threshold becomes larger, more pixel differences will be wrongly encoded as *uncertain* state, and the performance will drop as shown in Fig. 7(a). When the noise level is high, the pixel differences spread out and the histogram becomes flat. A large threshold is needed to handle the large image noise.

2) *Resistant to Additive Uniform Noise*: Uniform noise is another common type of noise. We conduct experiments on the AR database injected with additive uniform noise in the range of $(-p/2, p/2)$. The corresponding standard derivation is $\sigma_u = p/\sqrt{12}$. We vary the noise range for $p = 0.1, 0.2, 0.4, 0.7$, and respectively $\sigma_u = 0.0289, 0.0577, 0.1155, 0.2021$. Sample images are shown in Fig. 8. When the noise level is high, the images are severely distorted and barely recognizable.

The proposed approaches are compared with 6 LBP/LTP variants on the AR database injected with uniform noise. The average recognition rates and the standard derivation at the optimal setting are summarized in Table III. Both proposed

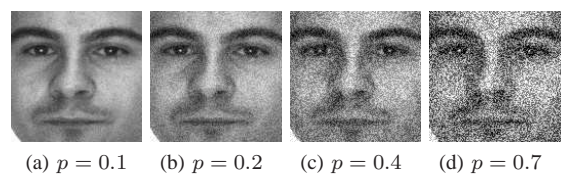


Fig. 8. The images with uniform noise of $p = 0.1, 0.2, 0.4, 0.7$, respectively.

approaches achieve comparable or better performance than other approaches. DLBP performs well for very low noise level, but it is even more sensitive to noise than LBP and hence performs even worse than LBP for middle and high noise levels. FLBP is also shown resistant to noise. Except for FLBP, as the noise level increases, the performance gain of the proposed approaches over other approaches increases.

B. Texture Recognition on Outex-13 dataset

Outex-13 dataset [40] consists of 68 classes of textures, each with 20 images. To test the noise-resistant property of the proposed approaches on the applications other than face recognition, we inject Gaussian noise and uniform noise of different noise levels onto the images of Outex-13 dataset, e.g. Gaussian noise of $\sigma = 0.05, 0.10, 0.15$ and uniform noise

TABLE III
SUMMARY OF THE AVERAGE RECOGNITION RATE AND THE STANDARD DERIVATION OF EACH APPROACH AT THE OPTIMAL SETTING ON THE AR DATABASE INJECTED WITH UNIFORM NOISE.

Algorithm	Chi-square Distance, $p =$				Histogram Intersection, $p =$				Modified G-Statistics, $p =$			
	0.1	0.2	0.4	0.7	0.1	0.2	0.4	0.7	0.1	0.2	0.4	0.7
LBP	87.57% ±1.37%	81.74% ±2.29%	53.81% ±9.01%	26.62% ±5.47%	87.13% ±1.13%	78.46% ±1.88%	45.85% ±11.55%	25.33% ±5.51%	84.94% ±1.30%	77.18% ±3.05%	46.24% ±7.50%	21.66% ±2.56%
LTP	87.83% ±1.07%	82.80% ±1.42%	62.27% ±4.52%	32.55% ±3.82%	87.50% ±1.13%	79.15% ±1.54%	48.41% ±12.91%	26.77% ±5.98%	85.20% ±1.27%	77.64% ±3.43%	54.56% ±4.60%	27.01% ±4.10%
DLBP	88.44% ±1.10%	83.25% ±1.26%	54.44% ±11.78%	24.79% ±6.28%	89.59% ±1.28%	82.72% ±1.78%	51.20% ±13.54%	24.39% ±8.19%	88.48% ±1.28%	81.42% ±1.37%	46.29% ±13.58%	8.92% ±1.61%
FLBP	87.23% ±1.33%	82.87% ±1.26%	75.26% ±2.04%	50.39% ±3.23%	87.11% ±1.22%	82.65% ±1.29%	68.53% ±3.07%	41.47% ±2.11%	85.25% ±1.31%	80.55% ±1.71%	72.31% ±2.16%	46.63% ±4.04%
NELBP	74.77% ±5.06%	60.00% ±5.33%	24.60% ±4.29%	15.52% ±4.26%	75.73% ±4.18%	58.14% ±4.66%	23.25% ±3.60%	15.83% ±3.55%	75.79% ±4.38%	60.56% ±4.57%	24.19% ±4.08%	15.16% ±3.61%
NTLBP	73.88% ±5.70%	57.35% ±3.19%	20.80% ±1.08%	8.67% ±1.29%	75.71% ±4.85%	62.39% ±2.77%	25.01% ±2.38%	11.09% ±1.67%	73.88% ±5.23%	54.07% ±4.04%	16.82% ±1.61%	7.61% ±1.26%
NRLBP	88.07% ±0.89%	84.48% ±1.09%	77.26% ±2.55%	56.07% ±5.15%	88.79% ±0.81%	85.06% ±1.10%	75.76% ±2.94%	53.61% ±6.95%	87.38% ±1.25%	83.90% ±0.80%	76.38% ±2.04%	55.90% ±4.94%
ENRLBP	88.68% ±0.91%	84.51% ±1.70%	77.37% ±1.46%	56.22% ±3.51%	88.89% ±0.89%	84.97% ±1.49%	76.09% ±2.16%	51.74% ±5.29%	87.81% ±1.15%	84.43% ±1.02%	76.99% ±1.05%	55.76% ±4.41%

TABLE IV
TEXTURE RECOGNITION ON THE OUTEX-13 DATABASE INJECTED WITH GAUSSIAN NOISE AND UNIFORM NOISE.

Algorithm	Gaussian Noise			Uniform Noise		
	$\sigma = 0.05$	$\sigma = 0.1$	$\sigma = 0.15$	$p = 0.1$	$p = 0.2$	$p = 0.4$
LBP	52.09% ±1.23%	41.71% ±0.96%	33.53% ±0.34%	65.21% ±1.01%	47.18% ±0.93%	38.26% ±0.99%
LTP	59.26% ±1.01%	50.85% ±1.16%	43.03% ±1.27%	69.74% ±1.07%	54.50% ±1.95%	51.74% ±2.10%
DLBP	52.47% ±1.02%	41.26% ±1.53%	32.74% ±1.38%	64.62% ±0.74%	47.00% ±1.20%	38.29% ±1.20%
FLBP	61.29% ±2.59%	53.32% ±1.58%	42.85% ±1.49%	69.56% ±0.96%	55.65% ±1.32%	52.53% ±1.55%
NELBP	34.50% ±1.83%	33.59% ±1.68%	26.76% ±0.68%	42.59% ±1.32%	29.76% ±1.46%	30.88% ±2.34%
NTLBP	32.09% ±2.26%	31.56% ±0.69%	26.68% ±1.19%	40.91% ±1.39%	27.00% ±0.76%	29.24% ±1.93%
NRLBP	62.88% ±0.95%	54.62% ±0.74%	43.24% ±1.00%	71.50% ±1.27%	58.15% ±1.09%	55.41% ±1.78%
ENRLBP	63.09% ±1.96%	55.06% ±1.66%	44.26% ±1.00%	70.94% ±1.15%	58.09% ±0.48%	54.76% ±0.58%

of $p = 0.1, 0.2, 0.4$. Preprocessing in [19] is useful to reduce noise. Thus, the noisy images are preprocessed in the same way as in [19]. Sample images and preprocessed images are shown in the first and second row of Fig. 9, respectively. We randomly choose 10 images from each class for training and the rest for testing. The proposed approaches are compared with 6 LBP/LTP variants. We extract features using 8 neighbors at the radius of one. Linear SVM is used as the classifier, which is implemented using LIBSVM package [45]. The cost parameter C is chosen as 1. The experiments are repeated 5 times, and only the average performance is reported. Table IV summarizes the performance comparison on the Outex-13 dataset injected with Gaussian noise and uniform noise. The proposed NRLBP and ENRLBP consistently achieve comparable or better performance compared with other approaches.

C. Face Recognition on the Extended Yale B Database

The extended Yale B database [41], [42] contains 38 subjects under 9 poses and 64 illumination conditions. We follow the same database partition as in [19]. The images with most neutral light source (“A+000E+00”) are used as the gallery images and all other frontal images are used as the probe images (in total 2414 images of 38 subjects). This dataset contains large illumination variations. The sample images are shown in the first row of Fig. 10. Some images are taken under extreme lighting conditions. Even after photometric

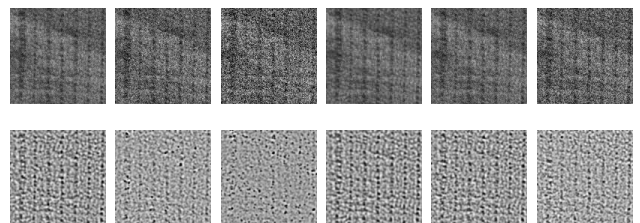


Fig. 9. Row 1 shows the sample images of Outex-13 dataset injected with Gaussian noise of $\sigma = 0.05, 0.10, 0.15$ and uniform noise of $p = 0.1, 0.2, 0.4$, respectively. Row 2 shows the respective images after the preprocessing as in [19].

normalization, as shown in the second row of Fig. 10, a large amount of image noise exist in the images. The proposed approaches are compared with 6 LBP/LTP variants using nearest-neighbor classifier with Chi-square distance, histogram intersection and modified G-statistic. Table V summarizes the highest recognition rates at the optimal threshold for various approaches using different distance measures. The proposed approaches achieve a slightly better performance than LBP, LTP, DLBP and FLBP, and much better performance than NELBP and NTLBP.

D. Face Recognition on the O2FN Mobile Database

The O2FN mobile face database [43] is our in-house face database. It is designed to evaluate the face recognition algo-

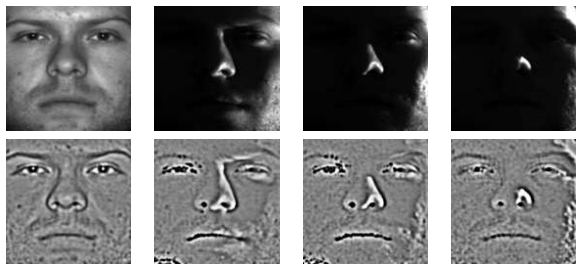


Fig. 10. The 1st row and 2nd row show the samples of geometrically normalized and photometrically normalized images for the extended Yale B database, respectively. The leftmost image is the gallery image, and the other 3 images taken under extreme lighting conditions are the probe images.

TABLE V

THE FACE RECOGNITION RATE AND THE OPTIMAL THRESHOLD ON THE EXTENDED YALE B DATABASE.

Algorithm	Chi-square Distance	Histogram Intersection	Modified G-Statistics
LBP	96.07%	93.32%	96.12%
LTP	98.25% (10)	97.99% (10)	98.29% (8)
DLBP	96.12%	97.83%	98.45%
FLBP	98.45% (9)	98.16% (9)	98.54% (12)
NELBP	81.91%	82.29%	84.92%
NTLBP	80.37%	80.16%	83.12%
NRLBP	98.71% (9)	98.66% (8)	98.66% (11)
ENRLBP	98.75% (9)	98.66% (8)	98.62% (10)

ritms on mobile face images, which are of low resolution and low image quality, and significantly corrupted by the noise. It contains 2000 face images of size 144×176 pixels from 50 subjects. The images are self-taken by the users. The users are told to take roughly 20 indoor images and 20 outdoor images with minimum facial expression variations and out-plane rotations. Thus, the O2FN database mainly contains in-plane rotations and illumination variations. Fig. 11 shows some samples of geometrically normalized and photometrically normalized images. The images are captured by O2 XDA frontal camera with native phone settings and without post-processing. The images are severely distorted by the noise, e.g. Gaussian noise, Salt & Pepper noise and motion blur. To reduce the noise and illumination variations, the images are photometric normalized as in [19]. Even after the photometric normalization, as shown in Fig. 11, the images still contain a large amount of noise.

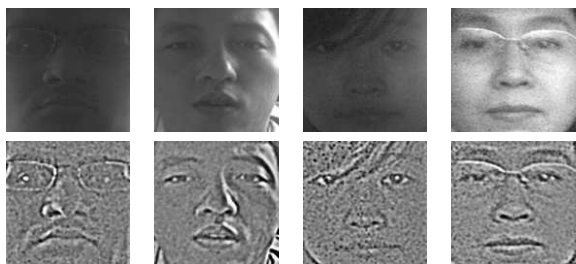


Fig. 11. The samples of geometrically normalized (Row 1) and photometrically normalized (Row 2) face images of the O2FN databases.

The proposed approaches are compared with 6 LBP/LTP variants using nearest-neighbor classifier with 3 different distance measures. The experiments are repeated 5 times. For

each trial, we randomly choose one image of each subject as the gallery set and the rest as the probe set. We test LTP, NRLBP and ENRLBP for different thresholds, and FLBP for different d . Only the performance at the optimal setting is reported. The average recognition rates and the standard derivation at the optimal setting on the O2FN database are summarized in Table VI. The proposed NRLBP and ENRLBP achieve a comparable or slightly better performance compared with LTP, DLBP and FLBP, and significantly outperform LBP, NELBP and NTLBP using all three distance measures.

TABLE VI
PERFORMANCE COMPARISON FOR FACE RECOGNITION ON THE O2FN DATABASE.

Algorithm	Chi-square Distance	Histogram Intersection	Modified Statistics	G-
LBP	76.59% \pm 1.60%	74.14% \pm 1.44%	75.18% \pm 1.15%	
LTP	78.88% \pm 1.65%	76.88% \pm 1.91%	78.16% \pm 1.39%	
DLBP	78.07% \pm 1.69%	79.88% \pm 2.10%	79.01% \pm 2.04%	
FLBP	80.24% \pm 1.58%	79.15% \pm 1.49%	80.01% \pm 1.46%	
NELBP	56.74% \pm 1.75%	58.25% \pm 2.16%	59.12% \pm 1.73%	
NTLBP	56.96% \pm 1.82%	58.40% \pm 1.65%	58.63% \pm 2.18%	
NRLBP	80.76% \pm 1.56%	80.29% \pm 1.63%	80.68% \pm 1.57%	
ENRLBP	81.66% \pm 1.83%	81.28% \pm 1.80%	81.44% \pm 1.91%	

E. Protein Cellular Classification on 2D HeLa Database

Protein cellular classification is useful when characterizing newly discovered genes. 2D HeLa database contains 862 single-cell images (16-bit gray scale of size 382×382 pixels) [44]. There are ten classes in this database and each with more than 70 images. Some sample images are shown in Fig. 12. Multi-

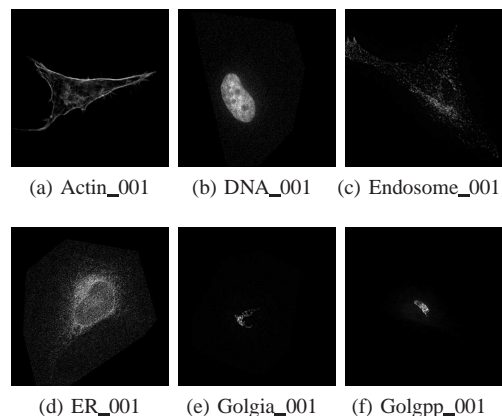


Fig. 12. Sample images of the 2D HeLa database.

scale LBP has shown good performance on this dataset [46]. We use $\{P, R\}$ to represent the descriptor extracted using P neighbors at the distance of R to the center pixel. Then, we extract features at multiple scales: $\{8, 1\}$, $\{8, 2\}$ and $\{8, 3\}$. Then those features are concatenated as the final feature vector for classification. Linear SVM [45] is used for classification. The cost parameter is the same as in [37], i.e. $C = 100$. We randomly choose 80% of the database for training and 20% for testing. The experiments are repeated five times and the average performance is reported. The performance comparison of the proposed approaches with other LBP/LTP variants are

shown in Table VII. The proposed NRLBP achieves the highest recognition rate of 95.93%. FLBP, LTP and the proposed ENRLBP also achieve good performance on this dataset.

TABLE VII
THE PERFORMANCE COMPARISON FOR PROTEIN CELLULAR CLASSIFICATION ON THE 2D HELA DATABASE IN TERMS OF RECOGNITION RATE AND TIME.

Algorithm	Average recognition rate	Time (ms)
LBP	89.53% \pm 0.41%	64.7
LTP	95.70% \pm 1.91%	95.5
DLBP	88.14% \pm 1.95%	109.2
FLBP	93.26% \pm 1.87%	2823.7
NELBP	91.16% \pm 1.04%	109.4
NTLBP	88.60% \pm 1.57%	110.3
NRLBP	95.93% \pm 1.48%	87.5
ENRLBP	95.58% \pm 0.66%	103.6

F. Image Segmentation

Besides recognition tasks, we also conduct comparison experiments for image segmentation. We extract features using 8 neighbors at the distance of one to the center. We follow the similar setup in [38] to segment texture images. Features are extracted in a raster-scanning way using sliding windows of 16×16 pixels with a step size of one pixel. K-means clustering algorithm with “cityblock” distance is used to classify the scanning windows. The number of clusters is given as input. Qualitative segmentation results of the proposed approaches and LBP/LTP variants are given. We choose the tenth image of the Outex segmentation test suite [40] and one natural scene image downloaded from the internet for illustration, as shown in Fig. 13 and Fig. 14. The Outex image consists of five textures. The ground-truth labeling of segments is shown in Fig. 13 (b). Apparently, the proposed NRLBP and ENRLBP achieve better segmentation performance than LBP, LTP, DLBP and FLBP. The natural scene image shown in Fig. 14(a) has four texture regions: sky, far forest, nearby forest and grassland. The proposed NRLBP and ENRLBP have much less misclassifications, and hence achieve better performance than other approaches.

G. Comparison of Computational Complexity

The proposed NRLBP and ENRLBP can be implemented by a look-up table to compute the NRLBP/ENRLBP histogram from the uncertain code. It is very fast to compute the contribution of an *uncertain* code to the histogram by the look-up table and hence derive the feature vector of NRLBP/ENRLBP during recognition. The average time per image of feature extraction on the 2D Hela database for various LBP/LTP variants is shown in Table VII. The image is of size 382×382 pixels. Features are extracted under the setting of $P = 8, R = 1$. We use Matlab 2012b on Intel Duo CPU 3.0 GHz with 4Gb RAM. Compared with LBP, NRLBP and ENRLBP only introduce a small overhead. NRLBP is in fact the second fastest approach. In contrast, it takes much more time to compute FLBP features, e.g. 2823.7 ms, which is 32 times of NRLBP.

IV. CONCLUSION

LBP is sensitive to noise. Even a small noise may change the LBP pattern significantly. LTP partially solves this problem by encoding the small pixel differences into the same state. However, both LBP and LTP treat the corrupted patterns as they are, and lack a mechanism to recover the underlining image local structures.

As the small pixel difference is most vulnerable to noise, we encode it as *uncertain* bit first, and then determine its value based on the other bits of the LBP code to form a code of image local structure. Uniform patterns represent local image primitives, and appear more frequently than non-uniform patterns in natural images. In contrast, non-uniform patterns are less reliable, thus are more error-prone. Therefore, we assign the values of *uncertain* bits so as to form all possible uniform LBP codes. In such a way, we correct noisy non-uniform patterns back to uniform code. For LBP and LTP, a large group of local primitives, i.e. line patterns, are completely ignored. Thus, we propose extended uniform patterns and form those patterns as our ENRLBP patterns when determine *uncertain* bits.

The proposed approaches show stronger noise-resistance compared with other approaches. We inject Gaussian noise and uniform noise of different noise levels on the AR database for face recognition and the Outex-13 dataset for texture recognition. Compared with FLBP, the proposed approaches are much faster and achieve comparable or slightly better performance. They consistently achieve better performance than all other approaches. We further compare the proposed NRLBP and ENRLBP with others for face recognition on the extended Yale B database and the O2FN database, protein cellular classification on the 2D Hela database, as well as image segmentation. The proposed approaches demonstrate superior performance on these applications.

ACKNOWLEDGMENT

This research is supported in part by the Singapore National Research Foundation under its International Research Centre @ Singapore Funding Initiative and administered by the IDM Programme Office.

REFERENCES

- [1] M. Inen, M. Pietikäinen, A. Hadid, G. Zhao, and T. Ahonen, *Computer Vision Using Local Binary Patterns*. Springer Verlag, 2011, vol. 40.
- [2] T. Ojala, M. Pietikäinen, and D. Harwood, “A comparative study of texture measures with classification based on featured distributions,” *Pattern recognition*, vol. 29, no. 1, pp. 51–59, 1996.
- [3] T. Ojala, M. Pietikainen, and T. Maenpaa, “Multiresolution gray-scale and rotation invariant texture classification with local binary patterns,” *IEEE Transactions on Pattern Analysis and Machine Intelligence*, vol. 24, no. 7, pp. 971–987, 2002.
- [4] B. Caputo, E. Hayman, and P. Mallikarjuna, “Class-specific material categorisation,” in *IEEE International Conference on Computer Vision*, 2005, pp. 1597–1604.
- [5] T. Ahonen and M. Pietikäinen, “Soft histograms for local binary patterns,” in *Proceedings of the Finnish signal processing symposium (FINSIG 2007)*, 2007, pp. 1–4.
- [6] —, “Image description using joint distribution of filter bank responses,” *Pattern Recognition Letters*, vol. 30, no. 4, pp. 368–376, 2009.
- [7] S. Liao, M. Law, and A. Chung, “Dominant local binary patterns for texture classification,” *IEEE Transactions on Image Processing*, vol. 18, no. 5, pp. 1107–1118, 2009.

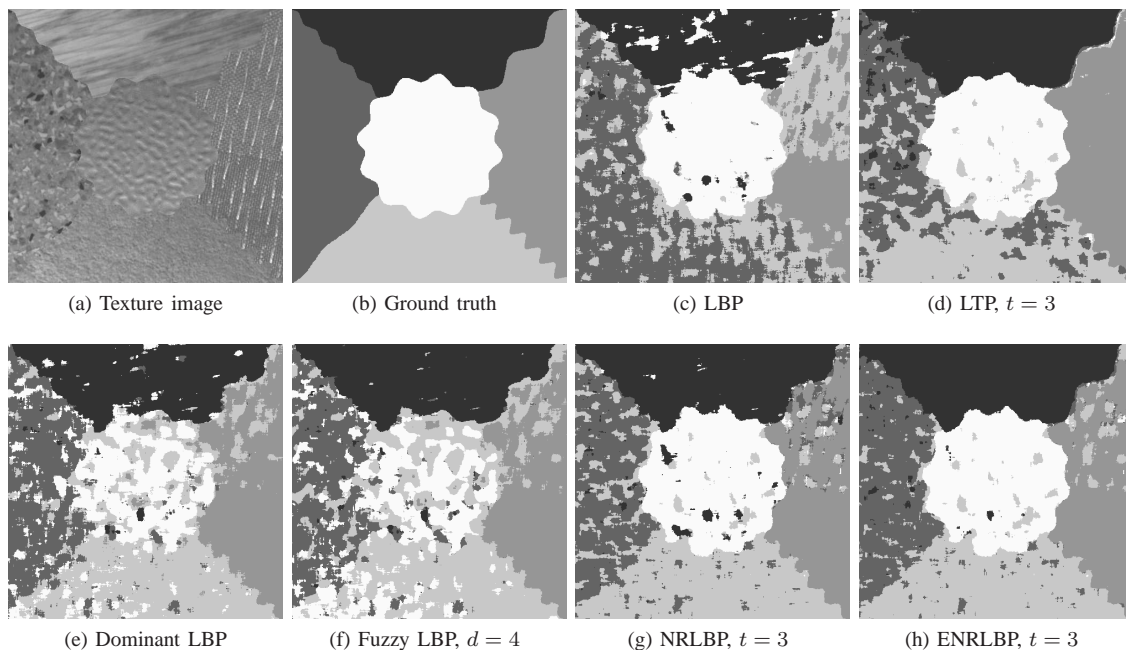


Fig. 13. Example of segmentation results on a mix-texture image for LBP, LTP, dominant LBP, fuzzy LBP, the proposed NRLBP and ENRLBP.

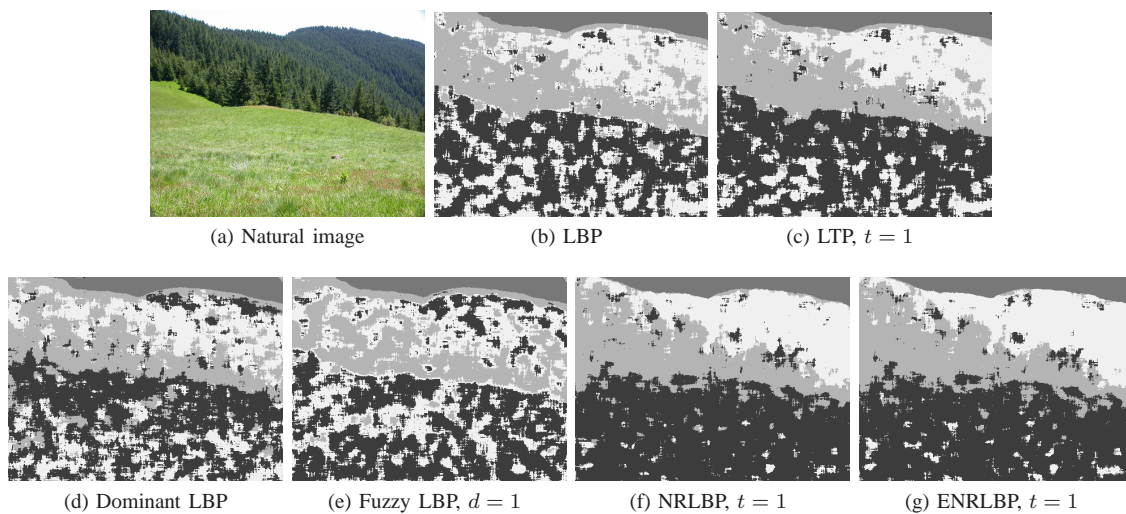


Fig. 14. Example of segmentation results on a natural scene image for LBP, LTP, dominant LBP, fuzzy LBP, the proposed NRLBP and ENRLBP.

[8] Z. Guo, L. Zhang, and D. Zhang, "A completed modeling of local binary pattern operator for texture classification," *IEEE Transactions on Image Processing*, vol. 19, no. 6, pp. 1657–1663, 2010.

[9] W. Liao and T. Young, "Texture classification using uniform extended local ternary patterns," in *2010 IEEE International Symposium on Multimedia (ISM)*. IEEE, 2010, pp. 191–195.

[10] Z. Li, G. Liu, Y. Yang, and J. You, "Scale-and rotation-invariant local binary pattern using scale-adaptive texton and subuniform-based circular shift," *IEEE Transactions on Image Processing*, vol. 21, no. 4, pp. 2130–2140, 2012.

[11] B. Ghanem and N. Ahuja, "Maximum margin distance learning for dynamic texture recognition," in *European Conference on Computer Vision*, 2010, pp. 223–236.

[12] G. Zhao and M. Pietikainen, "Dynamic texture recognition using local binary patterns with an application to facial expressions," *IEEE Transactions on Pattern Analysis and Machine Intelligence*, vol. 29, no. 6, pp. 915–928, 2007.

[13] G. Zhao, T. Ahonen, J. Matas, and M. Pietikainen, "Rotation-invariant image and video description with local binary pattern features," *IEEE Transactions on Image Processing*, vol. 21, no. 4, pp. 1465–1477, 2012.

[14] T. Ahonen, A. Hadid, and M. Pietikainen, "Face recognition with local binary patterns," in *European Conference on Computer Vision*, 2004, pp. 469–481.

[15] T. Ahonen, A. Hadid, and M. Pietikainen, "Face description with local binary patterns: Application to face recognition," *IEEE Transactions on Pattern Analysis and Machine Intelligence*, vol. 28, no. 12, pp. 2037–2041, 2006.

[16] S. Yan, H. Wang, X. Tang, and T. Huang, "Exploring feature descriptors for face recognition," in *Proc. IEEE International Conference on Acoustics, Speech and Signal Processing*, vol. 1, 2007, pp. 629–632.

[17] Y. Fang and Z. Wang, "Improving lbp features for gender classification," in *Proc. International Conference on Wavelet Analysis and Pattern Recognition*, 2008, pp. 373–377.

[18] N. Tan, L. Huang, and C. Liu, "A new probabilistic local binary pattern for face verification," in *Proc. IEEE International Conference on Image Processing*, 2009, pp. 1237–1240.

[19] X. Tan and B. Triggs, "Enhanced local texture feature sets for face recognition under difficult lighting conditions," *IEEE Transactions on Image Processing*, vol. 19, no. 6, pp. 1635–1650, 2010.

[20] M. Akhloufi and A. Bendada, "Locally adaptive texture features for

- multispectral face recognition," in *IEEE International Conference on Systems Man and Cybernetics (SMC)*. IEEE, 2010, pp. 3308–3314.
- [21] Z. Guo, L. Zhang, D. Zhang, and X. Mou, "Hierarchical multiscale lbp for face and palmprint recognition," in *Proc. IEEE International Conference on Image Processing*, 2010, pp. 26–29.
- [22] Y. Mu, S. Yan, Y. Liu, T. Huang, and B. Zhou, "Discriminative local binary patterns for human detection in personal album," in *Proc. IEEE Conference on Computer Vision and Pattern Recognition*, 2008, pp. 1–8.
- [23] X. Wang, T. Han, and S. Yan, "An hog-lbp human detector with partial occlusion handling," in *Proc. IEEE International Conference on Computer Vision*, 2009, pp. 32–39.
- [24] H. Jin, Q. Liu, H. Lu, and X. Tong, "Face detection using improved lbp under bayesian framework," in *Proc. International Conference on Image and Graphics*. IEEE, 2004, pp. 306–309.
- [25] H. Zhang, W. Gao, X. Chen, and D. Zhao, "Object detection using spatial histogram features," *Image and Vision Computing*, vol. 24, no. 4, pp. 327–341, 2006.
- [26] L. Zhang, R. Chu, S. Xiang, S. Liao, and S. Li, "Face detection based on multi-block lbp representation," *Advances in Biometrics*, pp. 11–18, 2007.
- [27] L. Nanni and A. Lumini, "Local binary patterns for a hybrid fingerprint matcher," *Pattern Recognition*, vol. 41, no. 11, pp. 3461–3466, 2008.
- [28] D. Iakovidis, E. Keramidas, and D. Maroulis, "Fuzzy local binary patterns for ultrasound texture characterization," *Image Analysis and Recognition*, pp. 750–759, 2008.
- [29] M. Heikkilä, M. Pietikäinen, and C. Schmid, "Description of interest regions with local binary patterns," *Pattern recognition*, vol. 42, no. 3, pp. 425–436, 2009.
- [30] D. He and N. Cercone, "Local triplet pattern for content-based image retrieval," *Image Analysis and Recognition*, pp. 229–238, 2009.
- [31] L. Nanni, A. Lumini, and S. Brahmam, "Local binary patterns variants as texture descriptors for medical image analysis," *Artificial intelligence in medicine*, vol. 49, no. 2, pp. 117–125, 2010.
- [32] S. Liao, G. Zhao, V. Kellokumpu, M. Pietikainen, and S. Li, "Modeling pixel process with scale invariant local patterns for background subtraction in complex scenes," in *IEEE Conference on Computer Vision and Pattern Recognition (CVPR)*. IEEE, 2010, pp. 1301–1306.
- [33] R. Gupta, H. Patil, and A. Mittal, "Robust order-based methods for feature description," in *IEEE Conference on Computer Vision and Pattern Recognition (CVPR)*, 2010, pp. 334–341.
- [34] H. Zhou, R. Wang, and C. Wang, "A novel extended local-binary-pattern operator for texture analysis," *Information Sciences*, vol. 178, no. 22, pp. 4314–4325, 2008.
- [35] A. Fathi and A. Naghsh-Nilchi, "Noise tolerant local binary pattern operator for efficient texture analysis," *Pattern Recognition Letters*, 2012.
- [36] J. Wu and J. Rehg, "Centrist: A visual descriptor for scene categorization," *IEEE Transactions on Pattern Analysis and Machine Intelligence*, vol. 33, no. 8, pp. 1489–1501, 2011.
- [37] L. Nanni, S. Brahmam, and A. Lumini, "A simple method for improving local binary patterns by considering non-uniform patterns," *Pattern Recognition*, vol. 45, no. 10, pp. 3844–3852, Oct. 2012.
- [38] E. Keramidas, D. Iakovidis, and D. Maroulis, "Fuzzy binary patterns for uncertainty-aware texture representation," *Electronic Letters on Computer Vision and Image Analysis*, vol. 10, no. 1, pp. 63–78, 2011.
- [39] A. Martinez and R. Benavente, "The AR face database," *CVC Tech. Report #24*, 1998.
- [40] T. Ojala, T. Maenpaa, M. Pietikainen, J. Viertola, J. Kyllonen, and S. Huovinen, "Outex-new framework for empirical evaluation of texture analysis algorithms," in *Proceedings of International Conference on Pattern Recognition*, vol. 1, 2002, pp. 701–706.
- [41] A. Georghiades, P. Belhumeur, and D. Kriegman, "From few to many: Illumination cone models for face recognition under variable lighting and pose," *IEEE Transactions on Pattern Analysis and Machine Intelligence*, vol. 23, no. 6, pp. 643–660, 2001.
- [42] K. Lee, J. Ho, and D. Kriegman, "Acquiring linear subspaces for face recognition under variable lighting," *IEEE Transactions on Pattern Analysis and Machine Intelligence*, vol. 27, no. 5, pp. 684–698, 2005.
- [43] J. Ren, X. Jiang, and J. Yuan, "A complete and fully automated face verification system on mobile devices," *Pattern Recognition*, vol. 46, no. 1, pp. 45–56, 2013.
- [44] M. V. Boland and R. F. Murphy, "A neural network classifier capable of recognizing the patterns of all major subcellular structures in fluorescence microscope images of hela cells," *Bioinformatics*, vol. 17, no. 12, pp. 1213–1223, 2001.
- [45] C.-C. Chang and C.-J. Lin, "LIBSVM: A library for support vector machines," *ACM Transactions on Intelligent Systems and Technology*,

vol. 2, pp. 27:1–27:27, 2011, software available at <http://www.csie.ntu.edu.tw/~cjlin/libsvm>.

- [46] Y. Guo, G. Zhao, and M. Pietikinen, "Discriminative features for texture description," *Pattern Recognition*, vol. 45, no. 10, pp. 3834–3843, 2012.



he joined BeingThere Centre, Institute of Media Innovation, NTU as a research associate. Currently he is pursuing Ph.D. in Electrical and Electronic engineering at NTU. His research interests include face recognition, general pattern recognition and computer vision.

Jianfeng Ren received the B.Eng from National University of Singapore, major in Communication and MSc from Nanyang Technological University (NTU), major in Signal Processing in 2001 and 2009, respectively. He received Professional Engineers Board Gold Medal for his outstanding academic results among all EEE MSc graduates in 2009. From 2003 to 2007, he was in industry sections. In Dec 2007, he joined NTU as a project officer, responsible for the development of the face verification system on mobile devices. In Sept 2011,



From 1998 to 2004, Dr Jiang was with the Institute for Infocomm Research, A*Star, Singapore, as a Lead Scientist and the Head of the Biometrics Laboratory, where he developed a system that achieved the most efficiency and the second most accuracy at the International Fingerprint Verification Competition (FVC'00). He joined Nanyang Technological University (NTU), Singapore, as a faculty member in 2004 and served as the Director of the Centre for Information Security from 2005 to 2011. Currently, he is a tenured Associate Professor in School of EEE, NTU.

Xudong Jiang (M'02-SM'06) received the B.Eng. and M.Eng. degrees from the University of Electronic Science and Technology of China (UESTC), Chengdu, China, in 1983 and 1986, respectively, and the Ph.D. degree from Helmut Schmidt University, Hamburg, Germany, in 1997, all in electrical engineering. From 1986 to 1993, he was a Lecturer with UESTC, where he received two Science & Technology Awards from the Ministry for Electronic Industry of China. From 1993 to 1997, he was a Scientific Assistant with Helmut Schmidt University.

Dr Jiang has published over hundred papers, where 16 papers in IEEE Journals: TPAMI (4), TIP (4), TSP (3), SPM, TIFS, TCSVT, TCS-II and SPL. He is the holder of seven patents. His research interest includes signal/image processing, pattern recognition, computer vision, machine learning, and biometrics.



Junsong Yuan (M'08) is currently a Nanyang Assistant Professor at School of EEE, Nanyang Technological University (NTU). He also serves as the Program Director of Video Analytics at Infocomm Center of Excellence, School of EEE, NTU. He received Ph.D. from Northwestern University, Illinois, USA and M.Eng. from National University of Singapore. He was selected to the Special Class for the Gifted Young of Huazhong University of Science and Technology and received a B.Eng. of Communication Engineering in 2002.

Dr. Yuan's research interests include computer vision, video analytics, visual search and mining, human computer interaction, biomedical image analysis, etc. He has published extensively in leading journals and conferences of computer vision, pattern recognition, data mining, and multimedia. He serves as editor, co-chair, PC member and reviewer of many international journals/conferences/workshops/special sessions. He received Outstanding EECS Ph.D. Thesis award from Northwestern University, and the Doctoral Spotlight Award from IEEE Conf. Computer Vision and Pattern Recognition Conference (CVPR'09). He has filed three US patents and two provisional US patents.